JOURNAL OF CATALYSIS 125, 501–513 (1990)

Scanning Tunneling Microscopy of Platinum–Rhodium Gauze HCN Catalysts

B. A. COWANS,* K. A. JURMAN,* W. N. DELGASS,* Y. Z. LI,† R. REIFENBERGER,† AND T. A. KOCH‡

*School of Chemical Engineering and †Department of Physics, Purdue University, West Lafayette, Indiana 47907; and ‡E. I. du Pont de Nemours & Company, Petrochemicals Department, Wilmington, Delaware 19898

Received March 6, 1990; revised May 16, 1990

Scanning tunneling microscopy provides resolution of topographical features from 1 to 100 nm on images of the surface structure of commercial PtRh gauze catalysts for HCN production. Estimates of the surface roughness based on the widths of height distributions calculated for these images suggest that the roughness on this scale changes with time on stream. Surface area enhancement on a 350-nm-length scale was observed to be as high as 100% for the roughest area but was generally less than 15%. Thus, crystallite growth on a larger length scale (i.e., >1000 nm) appears to be the primary source of the reaction-induced increase in the surface area of this catalyst system. STM observations of the structure around pits and of features on a 1-nm scale suggest that this technique can reveal important details of the initiation and mechanism of the surface roughening process in this system. Scanning Auger microprobe results suggest further that local surface composition may play a role in controlling surface topography.

INTRODUCTION

Platinum–rhodium gauze catalysts are of commercial importance for the production of both hydrogen cyanide by the Andrussow process and nitric acid via the oxidation of ammonia in the Ostwald process. Both processes induce a dramatic restructuring, or recrystallization, of the catalyst surface (*1–9*), but significant Pt losses are not observed in the HCN process due to lower oxygen partial pressures (*1*). Scanning electron microscopy has provided a detailed, micrometer-scale view of the restructured catalysts (*1, 3–9*). We have focused on the use of scanning tunneling microscopy (STM) to examine the submicrometer scale topography of HCN catalysts.

In the Andrussow process, methane, ammonia, and air are passed over the catalyst at very high velocity and a pressure slightly above 1 atm. The catalyst gauze pack is nominally a few millimeters thick but may be several meters in diameter in commercial reactors. The reaction is highly exothermic and a $1:1:1.3$ ratio of $CH_4:NH_3:O_2$ produces an adiabatic gauze temperature of about 1370 K (*10*). During the reaction-driven restructuring (*1*), the catalyst surface area increases approximately tenfold (*2, 7*) due to the formation of randomly oriented facets, pits, and deep channels.

There is evidence that the recrystallization involves transport of metal from grain boundaries to low-index faces (*1, 3, 5, 6, 9, 11*). Little is known, however, about the early stages of this process or its effect on local composition and catalytic activity, issues that may be critical for the eventual control of catalyst activity and longevity. With quantitative topographical mapping on the 0.1- to 1000-nm scale, STM affords a view of the microstructure of a conducting catalyst surface not possible only a few years ago. Indeed, applications of STM to surface defects (*12*), atomic scale roughness (*13–15*), and catalysts (*16, 17*) have begun to appear in the literature. Although the

0021-9517/90 $3.00

need for conducting samples limits the types of catalysts that can be studied by STM, future applications to nonconducting materials may be extended by novel modes of STM imaging (e.g., Ref. (18)) and particularly by the related method AFM, atomic force microscopy (*19, 20*).

Our objectives in the initial phase of this work have been to establish the feasibility of STM experiments on commercial catalysts, to determine whether the morphological features on a submicrometer scale contribute significantly to the overall surface area by examination of the surface roughness and the relative surface area enhancement using STM, and to examine the effect of time on stream on the catalyst microstructure.

Fresh and reacted catalyst gauzes have been examined by STM. In addition, we have measured the morphology and average composition of the gauze with scanning electron microscopy (SEM) and X-ray photoelectron spectroscopy (XPS). A scanning Auger microprobe (SAM) has been used to begin to examine variations in local composition and possible correlations between composition and structure.

EXPERIMENTAL METHODS

Catalyst samples. The catalyst gauze is composed of 10–60 layers of individual screens woven from 0.08-mm-diameter Pt–(10%)Rh wire. The gauzes used in this study were taken from either commercial or pilot scale reactors following 24-h or 6-month reaction periods. A "burned-through" region of gauze was also examined following an unspecified reaction time, and a fresh or unused gauze was examined for comparison. Unless specified, samples were obtained without knowledge as to the lateral or vertical location within the gauze pack. Further, the reaction history and postreaction environment of the catalyst had not been well-documented prior to analysis. Therefore, no special precautions, such as handling in an inert atmosphere, were used.

SEM. Scanning electron micrographs were obtained on a JEOL JSM 35 CF microscope operated at a beam voltage of 25 kV. Images were recorded on Polaroid-type 55 film. Crystallite dimensions were measured directly from these images.

STM. The "pocket-sized" scanning tunneling microscope used in this study was based on the design of Gerber *et al.* (*21*) and was operated in air. The microscope was normally operated in the constant-current mode with a tunnel current of 1 nA from the tungsten tip to the sample and a sample bias voltage of 650 mV. These tungsten tips were made by electrochemically etching 0.25-mm-diameter tungsten wire in a 1 *M* NaOH aqueous solution. A bias voltage of 11 V was applied between the carbon rod cathode and the tungsten wire anode. Etching was complete when hydrogen evolution ceased, indicating that the tungsten wire had broken contact with the solution.

To obtain STM images of the catalysts, we first moved the tip close to an individual wire in the gauze while sighting the approach through an optical telescope. Automated scanning was begun when a tunneling current was achieved. The small diameter of the wire and the roughness of the surfaces made achieving a stable image an arduous process and precluded taking large numbers of images for statistical purposes.

The characteristic thermal drift of the microscope was determined from atomic images of highly oriented pyrolytic graphite (HOPG) to be less than approximately 0.2 Å/s. The piezoelectric tripod was made from 3-mm-thick PXE 41 ceramic. The x and y calibration was obtained by measuring the periodicity of a 3600 line/mm holographic diffraction grating (*22*). The z calibration was determined by a precise measurement of the average length of the x and y piezos (l_{xy}) and the length of the z piezo (l_z). The z calibration was obtained by simply scaling the x–y calibration constant by the ratio of l_z/l_{xy}. Scans of the holographic grating showed no systematic distortion except for the inevitable thermal drift of the piezo tripod. The lack of distortion indicates that the x and y piezo lengths are the same to better than one part in 50, corresponding to an

estimate of about 2% for the maximum distortion possible due to the calibration procedure employed.

A reference plane is normally subtracted from the STM image to account for small thermal drifts and local surface orientation. This is accomplished by selecting three points on the raw STM image. If the vectors defining these points are given by $\mathbf{r}_i = a_i\hat{x} + b_i\hat{y} + c_i\hat{z}$ with $i = 1,2,3$ then the coordinates of an arbitrary vector $\mathbf{r}$ lying in the same plane are given by the equation $(\mathbf{r} - \mathbf{r}_1) \cdot (\mathbf{r}_2 - \mathbf{r}_1) \times (\mathbf{r}_3 - \mathbf{r}_1) = 0$. Using these equations, z_{ref} is calculated for each x,y point, and the height of the reference plane is subtracted from the measured z values. In this way, all STM data points are referenced to the desired plane and the small tilts in the raw STM image are eliminated.

XPS. X-ray photoelectron spectra were recorded on a Perkin–Elmer PHI 5300 spectrometer. The Mg (1253.6 eV)/Al (1486.6 eV) dual anode X-ray source was operated at 15 kV and 300 or 400 W. The spectrometer was calibrated by setting the binding energies of the Au $4f_{7/2}$ and Cu $2p_{3/2}$ levels to 84.0 and 932.7 eV, respectively. The full width at half maximum for Ag $3d_{5/2}$ level (368.4 eV) was 0.86 eV at 489 kHz at a pass energy of 8.95 eV for which all data were collected. Background pressure in the analysis chamber was always less than 1×10^{-9} Torr.

SAM. Scanning Auger multiprobe analysis was performed on a Perkin–Elmer PHI 660 spectrometer equipped with an Ar^+ ion sputter source. Auger spectra were recorded using a 20-kV electron beam approximately 0.5 μm in diameter both prior to and after Ar^+ion etching. The ion source produces a beam of 3-kV Ar^+ ions approximately 1 mm in diameter, i.e., much larger than the analysis area. Samples were sputtered for a total of 15 to 20 min at an estimated rate of 100–120 Å/min.

RESULTS AND DISCUSSION

Surface Morphology

Several factors have been shown to influence the restructuring process (*1, 6, 9*). For example, the amount of restructuring depends on the reactant composition. Further, the high rate of reaction produces a concentration gradient across the gauze pack. The amount of restructuring observed for a particular screen therefore depends upon its vertical position within the gauze pack. In fact, the first few screens from the top, or upstream side, of the gauze generally become so rough that it is nearly impossible to separate them. McCabe *et al.* (*6*) have observed in the Ostwald process that the amount of restructuring can also depend on the lateral position across the gauze pack under conditions where heat dissipation becomes a problem.

The SEM micrographs shown in Fig. 1 confirm that the samples we have examined are similar to those reported in the literature (*1–8*) Figure 1a shows a wire from the first screen in a gauze pack after 24 h in a pilot-scale reactor. Figure 1b shows a section of the 19th screen from the same gauze pack. The enormous differences in morphology clearly support the ideas that the restructuring process is reaction driven and that the reaction is nearly complete over the first few screens of the gauze pack. Our first objective has been to examine how topographical features on a submicrometer-length scale are related to changes on the length scale shown in Fig. 1.

The STM images in Figs. 2–4 demonstrate qualitatively how the roughness characteristics change with scale as well as the ability of the STM to image features with different spatial resolution. All of these images were obtained on the bottom screen of a commercial gauze pack used for 6 months. Figure 2 illustrates that significant surface roughness exists on an atomic scale. The image covers an area 250 × 250 Å (1 Å = 0.1 nm), with a total height variation of about 13 Å. Hösler *et al.* (*12*) have ascribed similar features to platinum clusters formed on carbon-contaminated surfaces at high temperatures following the decomposition of ethylene. As discussed later, carbon is also present on our catalyst surfaces and could contribute to the features seen in Fig. 2.

Another interesting topographical feature

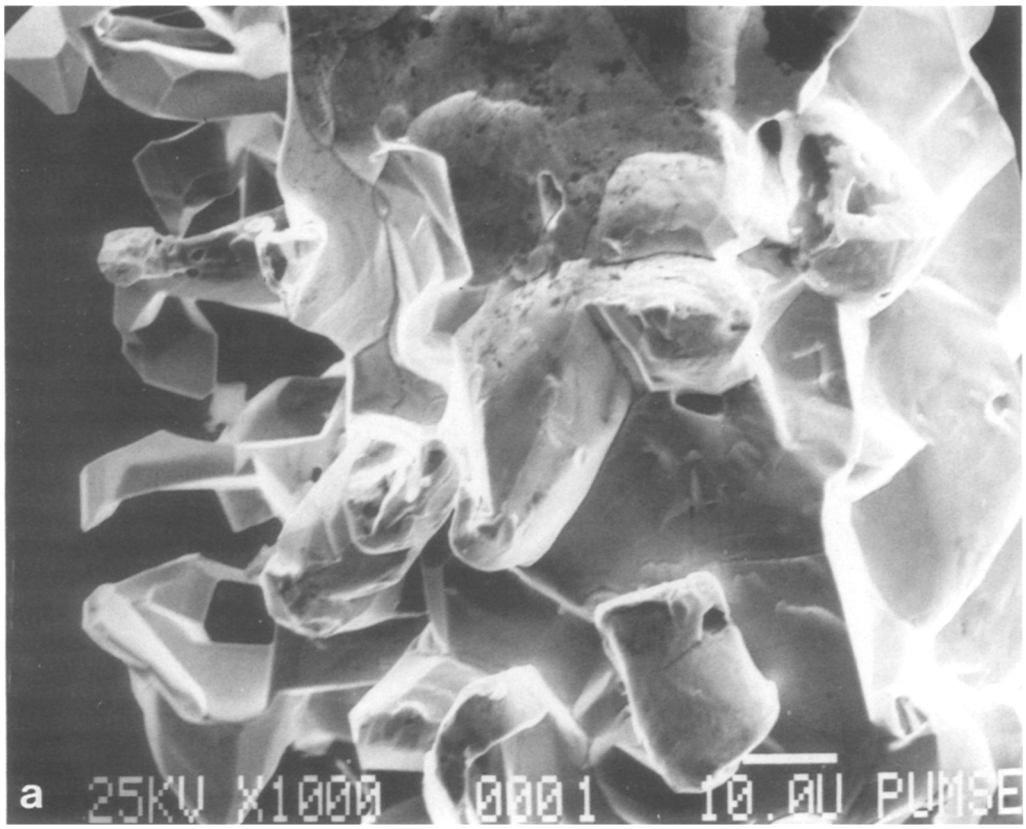

FIG. 1. Scanning electron micrographs (× 1000) of the first screen (a) and the 19th screen (b) of a PtRh gauze pack following 24 h of HCN reaction.

is shown in Fig. 3a where a small step about 8 Å high is observed on the catalyst surface in a 1000 × 1000 Å scan. Figure 3b, a 4000 × 4000-Å scan, shows another faceted region of the catalyst with steps approximately 20 Å high and plateaus roughly 2500 Å across. Regular atomic steps have been observed in images at several different scan sizes. The parallel nature of the steps suggests that they were formed by faceting in order to minimize the surface free energy of the catalyst ((Refs. (*3*, *9*) and references therein). It is not known when these steps form, but the fact that they continue uninterrupted across random distortions in the surface suggests that they are formed as the catalyst cools during quenching, rather than during reaction.

An estimate of the effective tip radius can be obtained by noting the rounding of the step edges due to tip-convolution effects. A straightforward analysis can be performed by realizing that even though the step edge will be distorted, the step height will remain unaffected by the finite radius of the tip. If it is assumed that a sharp step of height s is imaged by a tip with an apex that can be approximated by a sphere of radius R, then a geometrical analysis shows that the STM image of the step will be broadened by an amount related to the tip radius R and the step height s.

The worst distortion will be when $R \geq s$. Under these conditions, it is easy to show that w, the apparent step width measured from the STM scan, is given by $w = [s(2R$

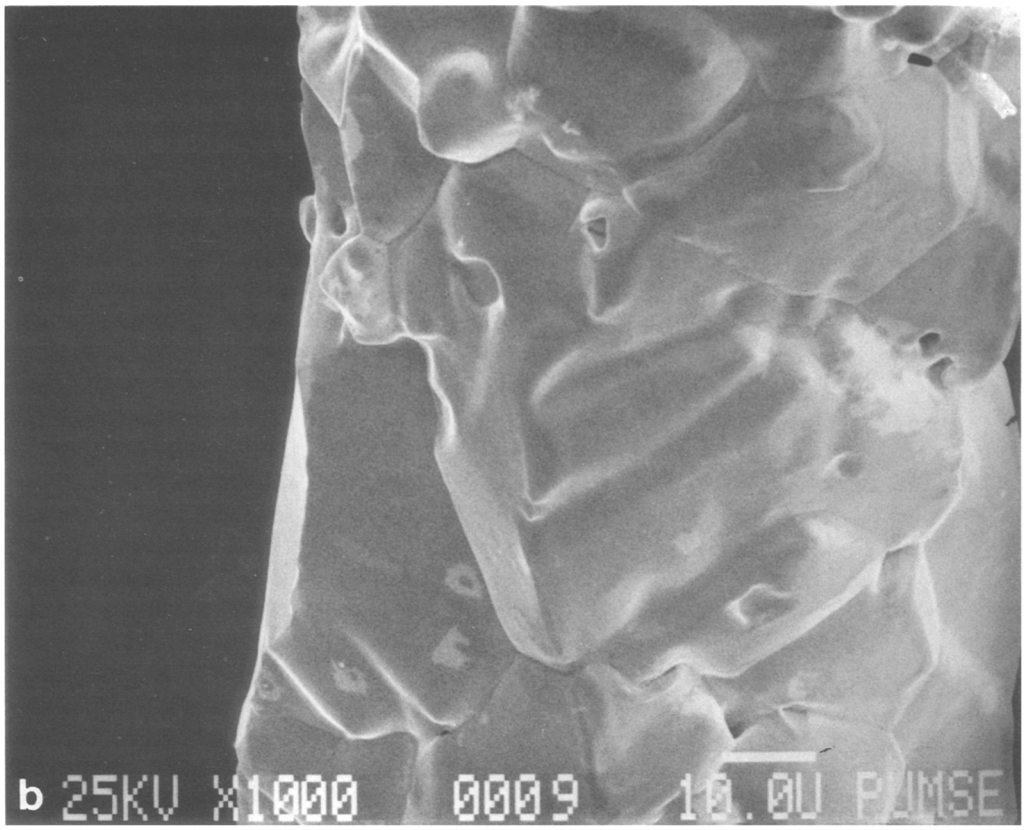

FIG. 1—*Continued.*

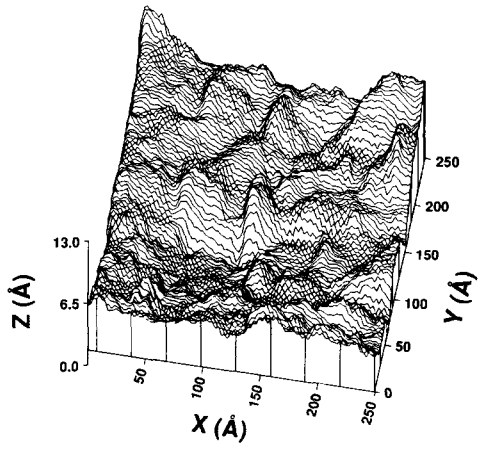

FIG. 2. STM image of surface roughness on the bottom screen of a 6-month PtRh gauze pack. Image covers 250 × 250 Å with a height variation of 13 Å.

$+ s)]^{1/2}$. For the steps observed above, the step width w was found to be smaller than the STM pixel size, δ. Using the worst case values of $w \leq \delta \cong 40$ Å, we find that $R \leq 20$ Å. This analysis provides an estimate for the geometry of the tips used in this study and suggests that the roughening features discussed below are not grossly misrepresented due to unwanted tip convolution effects.

Schmidt *et al.* (*3*) have observed by SEM that pit walls formed in Pt/Rh alloys during ammonia oxidation are generally faceted, that pit penetration is large relative to pit diameter, and that some metal appears to be deposited at the pit mouth. The 8000 × 8000 Å scan in Fig. 4 shows the presence of a large pit-like structure with similar charac-

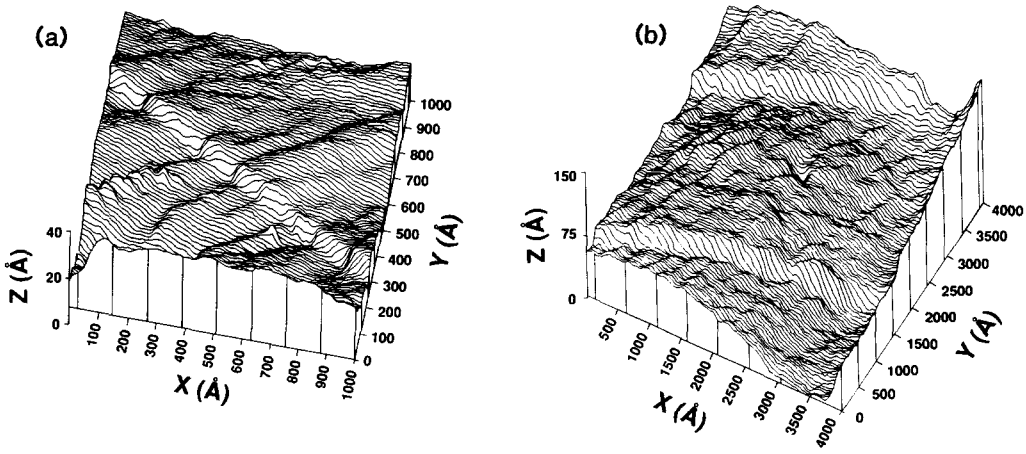

FIG. 3. STM images of faceted surfaces of a PtRh gauze used for 6 months. (a) A step 8 Å high; (b) steps 20 Å high.

teristics as well as the parallel step structure discussed above. In this case the steps are 20 Å high and approximately 4600 Å apart. The size of the pit in this image appears to be small relative to the amount of material around the pit mouth. Since penetration of the STM tip into the pit may be limited by the structure of the sides of the tip (*13*), the pit may actually be much deeper than is observed in this image. Although this pit is roughly one-tenth the size of those observed by Schmidt and co-workers, it is clear that material which appears to have come from within the pit is built up around the pit mouth.

A question of interest with regard to catalyst performance is whether the observed roughness on the STM scale makes a significant contribution to the surface area. We have begun to address this issue by developing two methods of analysis for describing the surface roughness observed in the STM images. The first method involves calculation of the relative surface area enhancement, as shown in Fig. 5. The topographical area is defined by calculating the two vec-

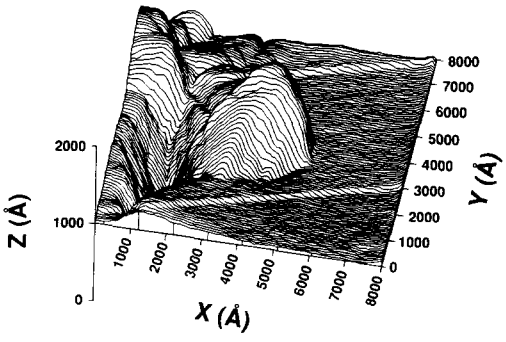

FIG. 4. An 8000 × 8000-Å STM image of a PtRh gauze used for 6 months showing pit structure with material deposited around the pit mouth.

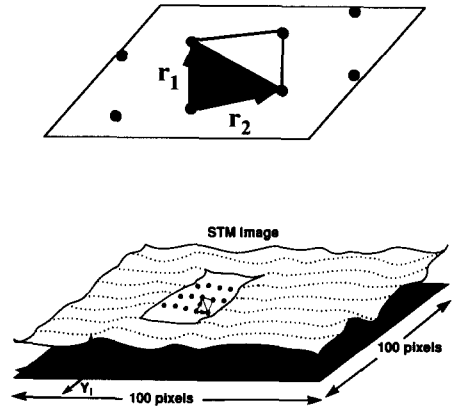

$$SA = 1/2\ (\vec{r}_1 \times \vec{r}_2)$$

FIG. 5. Illustration of the method used to calculate the relative surface area enhancement.

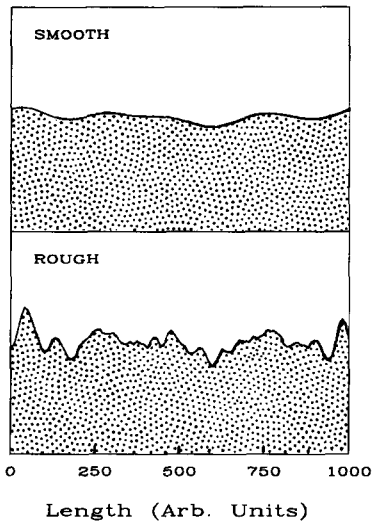

FIG. 6. Simulated smooth and rough surface profiles produced by three-point averaging a set of random numbers.

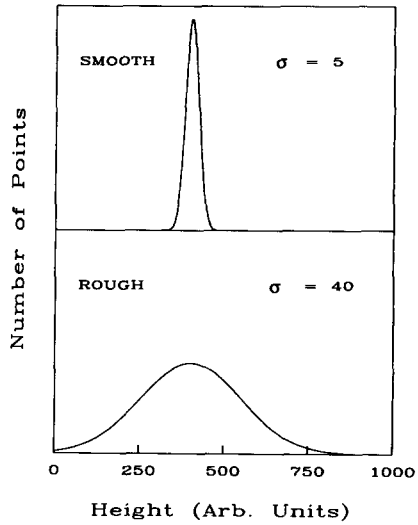

FIG. 7. Calculated standard deviations and height distributions for the simulated smooth (a) and rough (b) profiles in Fig. 6.

tors from data point $z(i,j)$ in the STM scan to the two points $z(i,j+1)$ and $z(i+1,j+1)$. The area of the triangle defined by these two vectors is one half the magnitude of the crossproduct of the two vectors. The total area is simply the summation, over all 10,000 points in the image, of these areas and the companion areas defined by $z(i,j)$, $z(i+1,j)$, and $z(i+1,j+1)$. The surface area enhancement, then, is the ratio of the topographical surface area divided by the area of a reference plane. Most of the area enhancements found thus far have been from 2 to 15%, although values as high as 100% have been seen.

The second method provides a measure of the actual surface roughness over a particular length scale. This is done by converting an STM image into a height distribution. The expected effects are illustrated schematically for one scan line in Figs. 6 and 7. Figure 6 was produced by three-point averaging a one-dimensional height profile simulated with a Gaussian random number generator. The smooth profile in Fig. 6a, produced after 50 averaging cycles, yields the narrow height distribution shown in Fig. 7a. The rough profile produced after only two averaging cycles is given in Fig. 7b. For convenience in analyzing STM images, we have used a Gaussian curve to fit the height distributions, as illustrated in Fig. 8. The standard deviation then provides a value that is related to the surface roughness. Interpretation of large standard deviation values may be complicated if the distribution

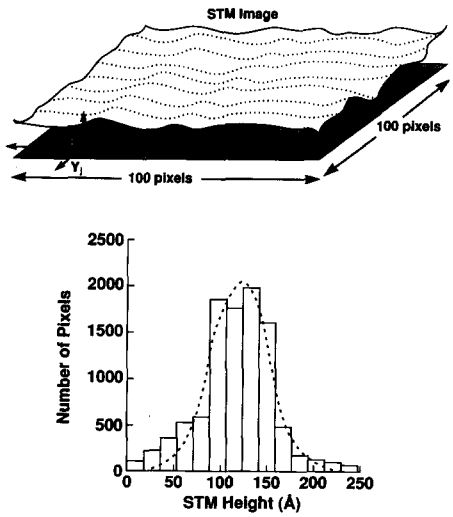

FIG. 8. Illustration of the method used to estimate the width of an STM height distribution.

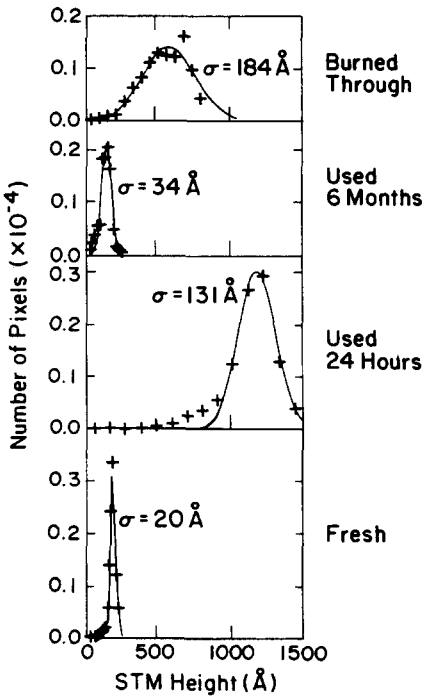

FIG. 9. Calculated height distributions for STM images of unreacted, 24-h, 6-month, and "burned-through" PtRh gauzes.

is bimodal, but, in general, increased breadth of the height distribution implies increased roughness.

Height distribution studies of the STM images for unreacted, used for 24 h, used for 6 months, and "burned-through" catalysts are shown in Fig. 9. Each distribution was calculated for a particular image that was representative of images obtained at random locations on the surface. A summary of all the height distributions calculated is given in Table 1.

Striations and pits were commonly observed on the unused, fresh catalyst and are apparently formed in the process of drawing the 0.08-mm wires. In the STM image, these features appear as channels approximately 100 Å deep and 180 Å across (*2, 8*). The increase in surface area, due mainly to these striations, is only about 3% and the surface roughness measurement shows a very narrow height distribution with an average standard deviation over all measurements of 28 ± 10 Å. These results indicate that the catalyst surface is initially very smooth.

As we have discussed, SEM images show that significant reconstruction occurs after only 24 h on stream. The STM images of some sections of this gauze show a tremendous number of pits and valleys that are several hundred angstroms across and sometimes over 1000 Å deep. The relative surface area calculated for such images is roughly a factor of 2 greater than that of a flat reference plane. Furthermore, the standard deviation of the height distribution is well over 100 Å, indicating a very rough surface. Since the interpretation of images having such large changes in height can be complicated by tip topography, electronic heterogeneity, and subsurface features such as caverns below holes in the surface, we conclude only that some regions of this surface are very rough. Other regions of this screen appear to be relatively smooth, with surface area enhancements and height distributions roughly the same as those for the unused catalyst. Finally, we note that the extremely rough regions of the type found on the used 24-h samples were not seen on any other samples.

After 6 months of reaction, the surface still appears quite rough on the 10-μm-length scale of the SEM images. All of the STM images, however, appear relatively smooth. Area enhancements were again calculated to be only about 3% larger than a flat reference plane and the average standard deviation dropped to 32 ± 5 Å. These results suggest that the surface has become quite smooth on the 3500-Å length scale.

The trend observed in the standard deviations of the height distributions for the unreacted, 24-h, and 6-month catalysts suggests that on a submicrometer scale the catalyst wires may initially roughen but become smooth again as the catalyst ages. This trend is quite interesting, but will require analysis of more samples of each type before it becomes statistically significant. For the most part, large standard deviations of the height

TABLE 1

Height Distribution Analysis

Catalyst	Area scanned (Å)	Number of measurements	Average σ
Fresh	1760 × 1760	3	35 ± 15
	3500 × 3500	5	24 ± 4
Used 24 h.	3500 × 3500	4	139 ± 83
Used 6 months	3500 × 3500	4	32 ± 5
"Burned through"			
Pit	3500 × 3500	2	179 ± 7
Smooth	3500 × 3500	2	38 ± 15

distribution appear to correlate with larger values of the surface area enhancement.

A "burned-through" or melted region of a catalyst contains very large holes which penetrate the entire gauze pack. These holes allow reactants to bypass the gauze pack, making the catalyst less effective. In general, the surface remains rough in the SEM images, while the STM images of this gauze are quite smooth. A rather interesting feature was observed by STM on this gauze and is shown in Fig. 10. This pit is more than 2000 Å across with a height variation of more than 800 Å. Note that the pit appears to be situated along a grain boundary and that material has again been built up around the pit mouth. This observation supports the hypothesis that migration of metal out of grain boundaries plays a role in the surface reconstruction process (*1, 3, 5, 6, 9, 11*). The area enhancement for this image is roughly 9%. The large standard deviation (184 Å) of the height distribution (see Fig. 9) for this image is caused by the fact that the dimensions of the hole are comparable to the scan size.

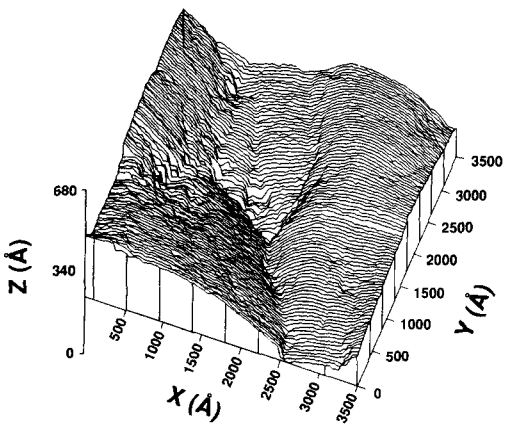

FIG. 10. STM image of pit structure apparently situated along a grain boundary.

The actual surface area of these wire gauze catalysts is quite difficult to measure accurately; however, areas measured by Anderson (*7*) using an electrochemical method and by Pan (*2*) using the BET method show roughly a tenfold increase in surface area during catalyst activation. The area enhancement observed on the STM scale is clearly not sufficient to account for this. A relatively simple model, similar to the "fuzzy" wire model used by Ray and Jensen to describe the oscillatory behavior of catalyst activities (*23*), can be used to simulate the increase in surface area due to changes in morphology resulting from crystallite formation. This analysis proceeds by initially modeling the unreacted catalyst as a cylinder with a diameter of 0.08 mm. As the restructuring progresses, a fraction of the total volume of the cylinder is converted to crystallites, modeled here as small cubes. An average length for the cube edge is obtained from the SEM micrographs and is generally between 10 and 30 μm (see also *Ref. (5)*). The cubes may be randomly oriented and are assumed to touch the surface of the now-smaller wire core at a single

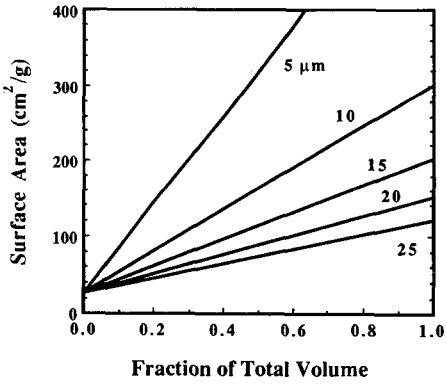

FIG. 11. The increase in surface area due to the fraction of the total volume of material converted to cubes. Each line represents a different cube edge length. Surface areas of 100–300 cm^2/g have been reported in the literature (*2*, *7*) for used catalysts.

point; i.e., the total surface area of each cube and the remaining wire core is exposed. The total surface area, then, is simply the sum of the surface areas of the cubes and the now smaller wire core. Applying the constraint that the total metal volume must be conserved, one finds that

$$A = A_0(1 - f)^{1/2} + 3A_0 f d_0/(2L), \quad (1)$$

where A is the surface area, f is the volume fraction of the original cylinder converted to cubes, d_0 is the diameter of the original cylinder, and L is the average length of a cube edge. In Eq. (1), the first term represents the area of the unreconstructed core and the second term the area of the cubes. Restructuring of the catalyst is complete when the total volume of the original cylinder is converted to cubes. This representation is quite reasonable since the large holes formed between crystallites often penetrate the entire diameter of the wire (*5*). The results of this simulation are presented graphically in Fig. 11. The value for A_0 (25 cm^2/g) used in this illustration was calculated for a smooth 0.08-mm wire and is in agreement with previous measurements for an unused gauze (*7*). Each line in the plot represents a different cube size. The areas calculated by this model for cubes with edge lengths less than 25 μm are comparable to the areas measured after reaction by Anderson (*7*) and Pan (*2*). As a consequence of this model and our STM observations, we propose that the surface area is composed of two components, a submicrometer component, which may account for as much as a factor-of-2 increase in area, and a micrometer scale component caused by crystallite formation, which is the major contributor to the observed increase in surface area.

Surface Composition

X-ray photoelectron spectroscopy has been used to study the average surface composition of these catalyst gauzes. Since the effective sampling area of the spectrometer is ~1 cm^2, the average is taken over several wires of the gauze. The depth of the measurement is governed by the mean free path for electron energy loss, about 20 Å. Representative platinum and rhodium spectra are shown in Fig. 12. Although a large amount of rhodium oxide has been observed on catalysts used in the Ostwald process (*4*, *6*, *8*),

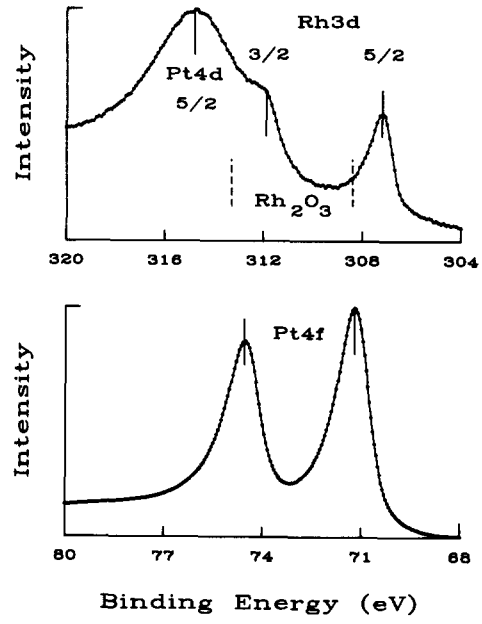

FIG. 12. Representative XPS spectra of the Rh 3*d* and Pt 4*f* regions of the PtRh gauzes.

TABLE 2

Relative Rhodium/Platinum Ratios from X-Ray Photoelectron Spectra[a]

Sample, position	(Rh $3d_{5/2}$)/(Pt $4f_{7/2}$)
Unused catalyst	0.140
Used 24 h, unknown	0.084
Used 24 h, screen No. 1	0.095
Used 24 h, screen No. 19	0.098
Used 6 months, unknown	0.079
Used 6 months, top screens	0.110
Used 6 months, bottom screens	0.087
"Burned-through" catalyst	0.091

[a] Ratios corrected for photoelectron cross-section.

the amount of oxidized rhodium observed on these catalysts is below the limits of detectability. This is consistent with the net reducing atmosphere in the Andrussow process, but may also be a function of the shut-down procedure (*24*). The relative ratios of rhodium to platinum are presented in Table 2 and are corrected only by Scofield's cross-sections (*25*). The relative surface concentration of Rh on the unused catalyst is higher than on any postreaction catalyst, as has been reported previously (*4*). This suggests that the catalyst preparation produces a surface slightly enriched in rhodium. Some slight variations in the Rh/Pt ratios are observed for the used catalysts. Most notable is the finding that the relative amount of platinum is only slightly lower on the top surface of a gauze pack after 6 months of reaction. These results show, as expected, that Pt is not volatile under HCN process conditions (*1*). XPS has also shown that a significant amount of carbon may be present on the catalyst surface, the equivalent of a 20- to 30-Å layer. We have not determined whether this is surface or interstitial carbon or whether it was deposited by the reaction or during shut-down; however, this result is compatible with observations made by Pan (*2*). We should also note that this intense carbon signal may be partially due to material trapped within the gauze pack.

Scanning Auger analysis was performed on the bottom screen of a gauze pack which had been used for 6 months in a commercial plant. This technique allows one to preview the potential importance of variations in the local surface composition, in this case on a 0.5-μm scale, with respect to changes in catalyst morphology. The SEM micrograph in Fig. 13 shows two of the areas that were analyzed by SAM. One area is relatively smooth, while the other area is covered with pits. The scanning Auger results confirm the presence of a large amount of carbon in both areas even after ion bombardment. The relative amount of carbon in the pitted area, however, is roughly double the amount observed in the smooth area. More importantly, the relative concentration of rhodium in the pitted area is only half that observed in the smooth area. These preliminary results suggest that correlations may exist between the relative rhodium and/or carbon concentration and the surface morphology.

CONCLUSIONS

We have found that we are able to obtain high-quality STM images of commercially used, and therefore macroscopically rough, catalysts that have undergone varying times of exposure to the reaction environment. These images clearly show microstructural details on a length scale that has not previously been accessible for study. Morphological changes seen at grain boundaries suggest that STM will be a useful tool for studying the initiation and propagation of the reaction-driven recrystallization. Quantitative analysis of the data suggests that roughness on a submicrometer-length scale changes substantially with time on stream, but contributes less than a factor of 2 to the total surface area of the catalyst. The major surface area changes can readily be accounted for by the formation of large crystallites. Measurement of surface roughness by the standard deviation of the height distribution correlates with the submicrometer-scale surface area enhancement, as expected. Although the surface of the unused catalyst

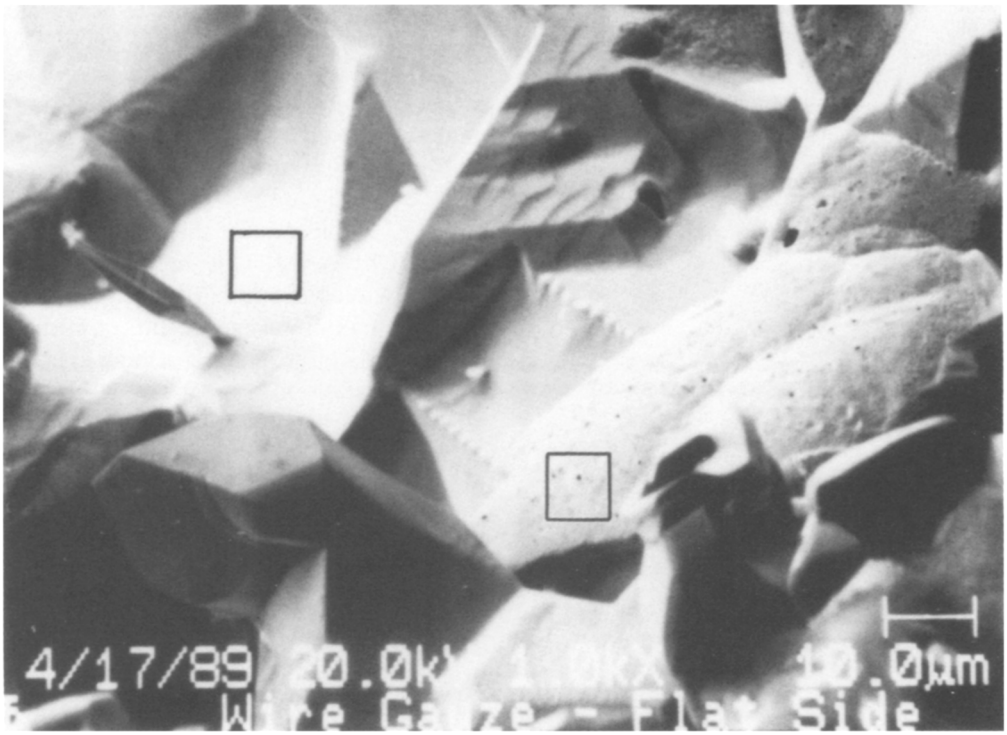

FIG. 13. SEM micrograph showing smooth and pitted regions analyzed by scanning Auger microprobe (SAM).

is somewhat enriched in rhodium, the relative platinum/rhodium composition does not change significantly over the lifetime of the catalyst. Scanning Auger results suggest, however, that local metal composition and carbon deposition vary with local topography.

ACKNOWLEDGMENTS

The authors would like to acknowledge support from E. I. du Pont de Nemours and Co. Quantitative analysis of STM images was assisted by R. C. Adams. SEM images were obtained with the assistance of L. D. McCabe in the School of Materials Engineering, Purdue University. Scanning Auger analyses were performed by Nancy Finnigan at the Center for Microanalysis of Materials, University of Illinois, which is supported by DOE under Contract DE-AC02-76ER 01198.

REFERENCES

1. Schmidt, L. D., and Luss, D., *J. Catal.* **22,** 269 (1971).
2. Pan, B. Y. K., *J. Catal.* **21,** 27 (1971).
3. McCabe, R. W., Pignet, T., and Schmidt, L. D., *J. Catal.* **32,** 114 (1974).
4. Contour, J. P., Mouvier, G., Hoogewys, M., and Leclere, C., *J. Catal.* **48,** 217 (1977).
5. Knapton, A. G., *Platinum Met. Rev.* **22,** 131 (1978).
6. McCabe, A. R., Smith, G. D. W., and Pratt, A. S., *Platinum Met. Rev.* **30,** 54 (1986).
7. Anderson, D. R., *J. Catal.* **113,** 475 (1988).
8. Fierro, J.L. G., Palacios, J. M., and Tomas, F., *Surf. Interface Anal.* **13,** 25 (1988).
9. Flytzani-Stephanopoulos, M., Wang, S., and Schmidt, L. D., *J. Catal.* **49,** 51 (1977).
10. Waletzko, N., and Schmidt, L. D., *AlChE J.* **34,** 1146 (1988).
11. Flytzani-Stephanopoulos, M., and Schmidt, L. D., *Chem. Eng. Sci.* **34,** 365 (1979).
12. Hösler, W., Behm, R. J., and Ritter, E., *IBMJ. Res. Dev.* **30,** 403 (1986).
13. Gimzewski, J. K., and Humbert, A., *IBM J. Res. Dev.* **30,** 472 (1986).
14. Denley, D. R., *J. Vac. Sci. Technol. A* **8,** 603 (1990).
15. Takeuchi, K., Uehara, Y., Ushioda, S., Mikoshiba, N., and Morita, S., *J. Vac. Sci. Technol. A* **8,** 557 (1990).
16. Schlögl, R., Wiesendanger, R., and Baiker, A., *J. Catal.* **108,** 452 (1987).

17. Komiyama, M., and Ogino, Y., *Shokubai* **31,** 84 (1989).
18. Kochanski, G. P., *Phys. Rev. Lett.* **62,** 2285 (1989).
19. Binnig, G., Quate, C. F., and Gerber, Ch., *Phys. Rev. Lett.* **12,** 930 (1986).
20. Weisenhorn, A. L., MacDougall, J. E., Gould, S. A. C., Cox, S. D., Wise, W. S., Massie, J., Maivald, P., Elings, V. B., Stucky, G. D., and Hansma, P. K., *Science* **247,** 1330 (1990).
21. Gerber, Ch., Binnig, G., Fuchs, H., Marti, O., and Rohrer, H., *Rev. Sci. Instrum.* **57,** 221 (1986).
22. Purchased from PTR Optics Corp., Waltham, MA.
23. Ray, W. H., and Jensen, K. F., *in* "New Approaches to Nonlinear Problems in Dynamics" (P. J. Holmes, Ed.), p. 235–255. SIAM, Philadelphia, 1980.
24. McCabe, A. R., and Smith, G. D. W., *Platinum Met. Rev.* **32,** 11 (1988).
25. Scofield, J. H., *J. Electron Spec. Relat. Phenom.* **8,** 129 (1976).